

Article

In Situ Experimental Study of Natural Diatomaceous Earth Slopes under Alternating Dry and Wet Conditions

Zhixing Deng ¹, Wubin Wang ^{1,2,*}, Tengfei Yan ¹, Kang Xie ³, Yandong Li ¹, Yangyang Liu ¹ and Qian Su ¹

¹ School of Civil Engineering, Southwest Jiaotong University, Chengdu 610031, China; 2020210063@my.swjtu.edu.cn (Z.D.); yantfxnjd@163.com (T.Y.); yandongli@my.swjtu.edu.cn (Y.L.); liuyy@my.swjtu.edu.cn (Y.L.); su1896swjtu@163.com (Q.S.)

² National Engineering Research Center of Geological Disaster Prevention Technology in Land Transportation, Southwest Jiaotong University, Chengdu 611731, China

³ Department of Civil Engineering, Central South University, Changsha 410075, China; xiekang1995@csu.edu.cn

* Correspondence: wangwubin.sju@outlook.com

Abstract: Very few studies have focused on diatomaceous earth slopes along high-speed railways, and the special properties of diatomaceous earth under alternating dry and wet conditions are unknown. This paper studies diatomaceous earth in the Shengzhou area, through which the newly built Hangzhou–Taizhou high-speed railway passes, and the basic physical and hydraulic properties of diatomaceous earth are analyzed by indoor test methods. A convenient, efficient, and controllable high-speed railway slope artificial rainfall simulation system is designed, and in situ comprehensive monitoring and fissure observation are performed on site to analyze the changes in various diatomaceous soil slope parameters under rainfall infiltration, and to explore the cracking mechanisms of diatomaceous earth under alternating dry and wet conditions. The results indicate extremely poor hydrophysical properties of diatomaceous earth in the Shengzhou area; the disintegration resistance index values of natural diatomaceous earth samples subjected to dry and wet cycles are 1.8–5.6%, and the disintegration is strong. Comprehensive indoor tests and water content monitoring show that natural diatomaceous earth has no obvious influence when it contacts water, but it disintegrates and cracks under alternating dry and wet conditions. The horizontal displacement of both slope types mainly occurs within 0.75–2.75 m of the surface layer, indicating shallow surface sliding; after testing, natural slope crack widths of diatomaceous earth reach 10–25 mm, and their depths reach 40–60 cm. To guarantee safety during high-speed railway engineering construction, implementing proper protection for diatomaceous earth slopes is recommended.

Keywords: high-speed railway; diatomaceous earth; dry and wet cycle; artificial rainfall simulation systems; in situ monitoring



Citation: Deng, Z.; Wang, W.; Yan, T.; Xie, K.; Li, Y.; Liu, Y.; Su, Q. In Situ Experimental Study of Natural Diatomaceous Earth Slopes under Alternating Dry and Wet Conditions. *Water* **2022**, *14*, 831. <https://doi.org/10.3390/w14050831>

Academic Editor: Stefano Morelli

Received: 31 January 2022

Accepted: 3 March 2022

Published: 7 March 2022

Publisher's Note: MDPI stays neutral with regard to jurisdictional claims in published maps and institutional affiliations.



Copyright: © 2022 by the authors. Licensee MDPI, Basel, Switzerland. This article is an open access article distributed under the terms and conditions of the Creative Commons Attribution (CC BY) license (<https://creativecommons.org/licenses/by/4.0/>).

1. Introduction

As of the end of 2020, China's operating railway mileage had reached 146,000 km, of which 37,900 km were high-speed railways. As the density of high-speed railway networks increases, high-speed railway construction will inevitably pass through special land areas. The newly built Hangzhou–Taizhou high-speed railway passes through Shengzhou city. A large amount of diatomaceous earth is present in the tertiary basalts and lacustrine deposits in the basalt platform area. Diatomaceous earth has well-developed joints, and is highly compressible; it easily softens when exposed to water, and its mechanical properties decrease substantially. Diatomaceous earth is in a hard-plastic-to-plastic state, and its engineering properties are extremely poor [1–6]. During on-site construction, diatomaceous earth slopes are exposed to the natural environment after excavation. The permeability coefficients of undisturbed diatomaceous earth are less than 10^{-6} cm/s, signaling an impervious layer in a given project. However, under alternating wet and dry conditions, depths of 40 to 60 cm are affected by the environment, resulting in cracks that greatly affect

the safe development of railway construction. Therefore, under the action of alternating wet and dry conditions, the destruction mechanism of diatomaceous earth and the dynamic evolution of diatomaceous earth slope parameters have become issues that urgently need to be studied.

At present, diatomaceous earth is widely used for environmental protection, and in chemical, electrical, and other fields, because of its high porosity and light weight [7–11]. However, the existing literature contains very few studies on diatomaceous earth slopes, and the special properties of diatomaceous earth under the action of dry and wet cycles are not well understood. On loess and expansive soil slopes, a lot of work has been done by scholars in the past; there is deeper research on the special properties of loess and swelling soil under the action of alternating wet and dry conditions, and a lot of practice has been done in combination with actual slope engineering; the main research results are shown in Table 1.

Table 1. Literature review table.

N°	Reference	Research Methods and Content	Research Findings
1	[12]	Artificial rainfall simulation experiments were conducted on loess slopes to study the damage mechanism of landslides under rainfall conditions.	Rainfall and landslides on loess slopes have a time lag.
2	[13]	The changes in shear strength, cohesion, and internal friction angle of loess samples under different dry and wet cycles were determined by indoor direct shear tests.	Under the same dry–wet cycle conditions, the larger the variation range of the water content, the lower the shear strength of the loess sample appears to be.
3	[14]	The influence of pore water pressure on the stability of loess slopes was analyzed by combining field monitoring and laboratory tests.	Rainfall can reduce the stability of loess slopes.
4	[15]	Indoor tests on loess soils were conducted.	The permeability coefficient of loess increases after dry–wet cycling, and the dry–wet cycling action causes damage to the microstructure of loess.
5	[16]	Indoor dry and wet cycle tests were conducted on expansive soils.	The shear strength of expansive soil decreased with the increase in the number of cycles, and finally reached a constant state
6	[17]	Indoor tests on natural expansive soils were conducted in Nanning.	The effective cohesion, which is an important factor affecting the occurrence of surface damage on expansive soil slopes, was reduced.
7	[18]	Centrifugal model tests were conducted on swelling soil slopes to analyze the changes in slope settlement, horizontal displacement, damage mechanism, and accumulated cracks under alternating wet and dry conditions.	The accumulation of cracks caused by dry–wet cycles is key to the progressive failure of slopes.
8	[19]	The variation patterns of shear strength parameters of expansive soils under different dry and wet cycles were analyzed by indoor tests.	The shallow damage of the expansive slope was mainly caused by the dry and wet effects of the natural environment.

A few studies have found that diatomaceous earth has high structural strength and is susceptible to disintegration and deterioration when exposed to water [20–24]. These properties derived from previous studies are slightly similar to those of loess and expansive soils, but are for reference only, and are not fully applicable to the field of high-speed railroad diatomaceous earth slopes. Meanwhile, compared with loess and expansive soil slopes, there are very few studies on diatomite slopes at home and abroad, and they are mainly concentrated in the fields of highway and marine engineering. For example, Zhang [22] conducted an in-depth study on the swelling properties of diatomite distributed in Tengchong, Yunnan, and showed the existence of light-swelling diatomite with strong swelling and disintegration in the area. Guo [25] studied the distribution characteristics and formation mechanisms of diatomite (soil) landslides by taking the new Tenglu highway slope landslide as an example, and pointed out that diatomite slopes are susceptible to cracking, delamination, and reduction in mechanical properties of diatomite on the slope

surface under the influence of artificial disturbance and external rainfall, etc. Wiemer [26] et al. studied the effect of diatoms on the shear strength of diatom sediments and the stability of submarine slopes, and pointed out that the shear strength of the diatom soil layer would be reduced under the condition of disturbance. Currently, no corresponding research results have been found in the field of high-speed railways, and there is no better solution for the damage problem of diatomaceous earth slopes under the alternating action of wet and dry conditions.

To gain a more thorough understanding of the diatomaceous earth slope damage caused by alternating dry and wet cycles, a research project was carried out for the diatomaceous earth in the Shengzhou area along the new Hangzhou–Taizhou high-speed railway. The study was performed through indoor testing, analysis of physical and hydraulic properties, and evaluation of the mechanisms of disintegration and degradation. Because previous rainfall simulation equipment cannot undertake the problem of rapid rainfall on high-speed railway slopes, a convenient, efficient, and controllable high-speed railway slope artificial rainfall system was designed, and alternating dry–wet cycle simulations were carried out on the test site. At the same time, in situ comprehensive monitoring and fissure observation were carried out before and after the alternating dry–wet simulations of natural diatomaceous earth slopes, in order to analyze the changing patterns of various diatomaceous earth slope parameters under rainfall infiltration conditions and explore the disintegration and cracking mechanisms of diatomaceous earth under the action of dry–wet cycles.

2. Project Overview

The diatomaceous earth natural slope test site was located between Dongdawan village and Xibanban village, on Lushan Street, in Shengzhou city, and next to Shangdawan Reservoir. To study the engineering characteristics of diatomaceous earth and the damage mechanism of diatomaceous earth under the action of dry–wet cycles, a diatomaceous earth cutting slope with mileage of DK85 + 824 – DK85 + 840 was selected as the test section (Figure 1a). The test section was covered with silty clay with a thickness of less than 3 m, and the underlying white diatomaceous earth was 9–12 m thick. The strata below the white diatomaceous earth were blue diatomaceous earth, black diatomaceous earth, basalt, stomatal basalt, and diatomaceous earth sandstone. After the excavation of the slope, the exposed surface and the depth interval of 10–27 m were mainly white diatomaceous earth (Figure 1b,c). Therefore, the properties of diatomaceous earth listed in this article and related tests are all white diatomaceous earth.



(a)

Figure 1. Cont.

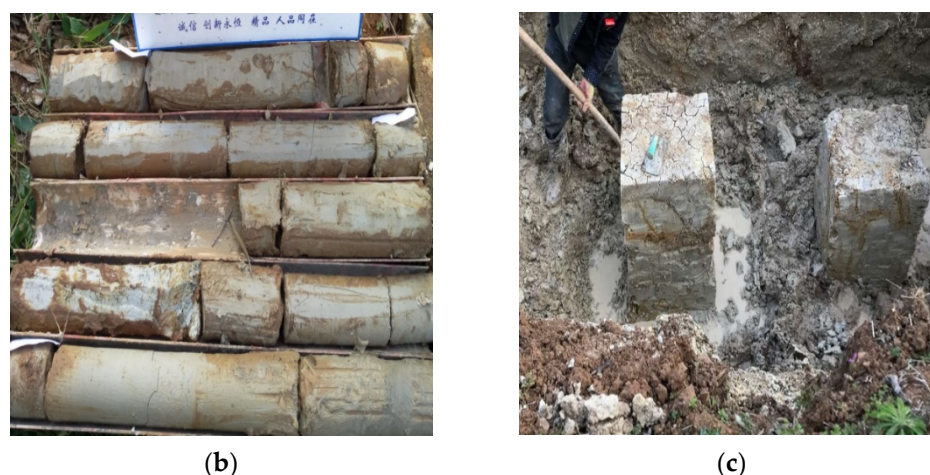


Figure 1. Test site and white diatomaceous earth: (a) Shengzhou diatomaceous earth slope test section; (b) white diatomaceous earth; (c) white diatomaceous earth drilling and construction.

3. Diatomaceous Earth Characteristics

Studies have found that diatomaceous earth has the undesirable property of degradation when in contact with water. To understand the mechanisms of diatomaceous earth's disintegration and degradation, an outdoor observation test of natural diatomaceous earth slopes was first carried out. Part of the cutting slope of the test section was graded with a slope ratio of 1:1.5. However, after a period of alternating dry and wet action, penetrating cracks were generated, and the depths of the cracks were between 0.5 and 0.8 m, as shown in Figure 2.

To solve the problem of damage to diatomaceous earth slopes under the action of dry and wet cycles, diatomaceous earth in the slope test section was used as the research object. First, basic geotechnical tests were carried out so as to become familiar with the basic physical properties of the diatomaceous earth in the area. Then, through water immersion observation and disintegration tests, the changes in diatomaceous earth after exposure to water were assessed, and the mechanisms of its disintegration and deterioration were initially evaluated.



Figure 2. Slope failure problem: (a) natural slope with a slope ratio of 1:1.5; (b) penetrating cracks that appear under the alternating action of dry and wet conditions.

3.1. Basic Physical Properties of Diatomaceous Earth

By taking samples at different depths at the foot of the natural slope on the right side of the line, ~155 m from the test slope, the original site was wax-sealed in time, and anti-vibration and sun protection measures were taken during transportation to ensure that the

original sample was not disturbed and did not lose water. Corresponding physical property tests were performed on the samples in time, in accordance with the “Geotechnical Test Procedure for Railway Engineering” [27]. In this study, white diatomaceous earth was used as the main research object, and representative samples were selected for corresponding tests. The properties of diatomaceous earth in this test section are shown in Table 2. Due to the large number of test results, it is inconvenient to list the specific data in each group. Through sampling at different depths, the results show that the natural density values of the diatomaceous earth were 1.55–1.73 g/cm³, which are extremely low, and are similar to those of pumice. The void ratio and water content of the diatomaceous earth samples were very high. The void ratios of the seven samples were all greater than 1.0; the maximum water content was 72.11%, and the average value was 55.78%. The diatomaceous earth was dominated by the particle size ranges of 0.075–0.005 mm and < 0.002 mm, with a combined fraction of 80%, and the proportion of particles in the particle size range of 0.25–0.075 mm was the lowest. The mean plasticity index value of diatomaceous earth specimens was 36.30, which was much larger than 10, so it was classified as clay.

Table 2. Basic physical properties and particle analysis of diatomaceous earth.

N°	—	Basic Physical Properties							Particle Size Range (mm)				
		Density (g/cm ³)	Dry Density (g/cm ³)	Water Content (%)	Void Ratio	W _p (%)	W _L (%)	I _p	0.50–0.25 (%)	0.25–0.075 (%)	0.075–0.005 (%)	0.005–0.002 (%)	<0.002 (%)
1	Maximum value	1.73	1.58	72.11	1.70	46.45	92.88	49.30	17.1	9.7	54.3	40.9	65.1
2	Minimum value	1.55	0.64	46.66	1.13	40.60	73.80	32.65	0.1	0.3	21.4	8.9	18.7
3	Average value	1.63	1.11	55.78	1.36	42.98	79.28	36.30	2.9	2.1	35.6	16.3	44.0
4	Number of groups	7	7	6	8	7	7	7	8	8	8	8	8

3.2. Hydrological Properties of Diatomaceous Earth

Ten samples of white diatomaceous earth collected in the field test section were divided into two groups with variable water contents. Each group consisted of five samples. The average mass of the samples was consistent with the disintegration test (151.22 g). The first group was left untreated, keeping each sample in its natural state. The second group was placed in a cool place in the laboratory to undergo the drying process. The test phenomena are shown in Figure 3. The natural diatomaceous earth had no obvious change after being immersed in water, and only a small amount of soil fell off on the surface. After the natural diatomaceous earth dried in the shade, cracks appeared, and then it was soaked in water. Because of its small specific gravity, the sample floated on the water for a few seconds, sank under the water, and quickly disintegrated into a fine scaly and powdery form.

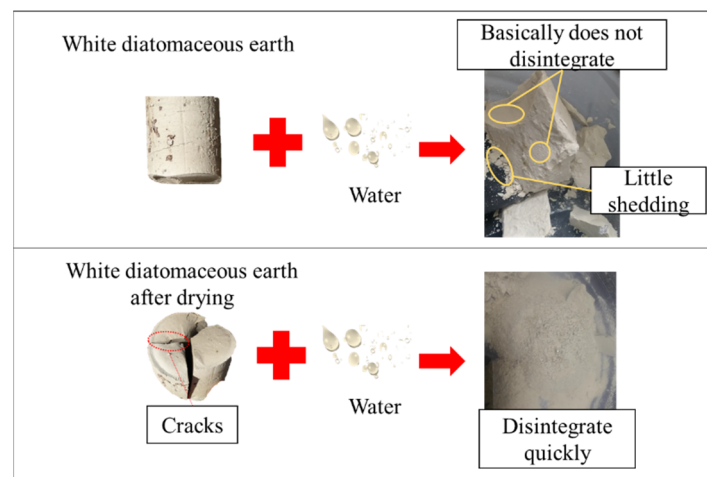


Figure 3. Natural diatomaceous earth and natural diatomaceous earth after shade-drying to observe the phenomenon of water immersion.

According to the above test phenomena of diatomaceous earth after encountering water, natural diatomaceous earth experiencing no obvious impact after encountering water. When natural diatomaceous earth dries, cracks appear and fragmentation occurs; then, the diatomaceous earth disintegrates quickly when exposed to water. The main reasons for this damage are as follows:

1. Natural diatomaceous earth has a high water content. In a natural environment or under high temperatures, due to the existence of a large number of clay minerals in the sample that are prone to strong shrinkage, the sample dries and shrinks [22,28]. At the same time, the shallow free water continues to evaporate, and air begins to enter the pores of the shallow soil particles, causing matrix suction between the particles on the soil surface. As water continues to evaporate, the suction of the matrix gradually increases, and the force on the soil particles becomes increasingly strong. When there are impurities or stress concentrations on the surface of the diatomaceous earth, the tensile strength of the diatomaceous earth is insufficient, and initial cracks are formed on the surface [29,30];
2. Since natural diatomaceous earth has a high void ratio and high water content, the dry density is significantly lower than the natural density, so the sample floats on the water surface for several seconds after the dry diatomaceous earth is immersed in water;
3. The natural diatomaceous earth that was dried in the shade forms cracks due to the above reasons. After being immersed in water, the water can dissolve and soften certain minerals in diatomaceous earth, resulting in further enlargement of the cracks and weakening of the connections between the soil particles. Then, because clay minerals such as montmorillonite and kaolinite swell because of water, the tensile strength of diatomaceous earth at the joints or microcracks is not enough to overcome the swelling force, leading to its rapid disintegration [31,32].

Through the abovementioned water immersion observation test, the state of diatomaceous earth after immersion in water is initially assessed. To further analyze the properties of diatomaceous earth after encountering water, two sets of white diatomaceous earth disintegration tests were designed. There were five samples in each group, and the average mass of the two groups of samples was 151.22 g. The effect of time and the total amount of disintegration and disintegration resistance of the two groups of samples under alternating natural dry and wet conditions when exposed to water were tested.

The diatomaceous earth sample was placed into a water-permeable sample box and immersed in a water tank to disintegrate. The mass of the residual sample was weighed with an electronic balance, and the ratio of the residual mass of the sample after disintegration to the total mass of the sample—that is, the disintegration resistance index (%)—was used to evaluate the disintegration characteristics of each sample.

$$I = \frac{M_r}{M_t} \times 100\% \quad (1)$$

where I is the resistance to disintegration index (%), M_r is the mass of the residual sample (g), and M_t is the total mass of the sample (g).

The test results are shown in Figure 4, and are summarized as follows:

1. The disintegration resistance index values of diatomaceous earth samples under natural conditions range from 89.6% to 92.8%, with an average value of 91.2%. The disintegration resistance index values of the sample after drying and wetting are 1.8–5.6%, and the average value is 3.7%. The comparison shows that the disintegration resistance index values of the natural diatomaceous earth samples are much higher than those of the diatomaceous earth samples after drying and wetting, and the drying and wetting effect has a great influence on the disintegration resistance of diatomaceous earth;

2. The water physical properties of the diatomaceous earth are extremely poor. The maximum disintegration resistance index value of the diatomaceous earth sample after alternating wet and dry action is 5.6%, which indicates extremely strong disintegration. The disintegration resistance of the sample is lower than that of soils with common parent rocks, such as basalt residual soil, mudstone, and granite [33–37];
3. The disintegration rate of the diatomaceous earth sample after alternating wet and dry conditions is lower in the first 30 s of being placed into the water. This phenomenon occurs because water gradually enters the pores of the sample during this period, and some of the air is surrounded by water in the pores. The high-speed disintegration of the sample occurs within 1–2 min after the start of the test, after which the disintegration rate decreases and tends to stabilize until the end of the test.

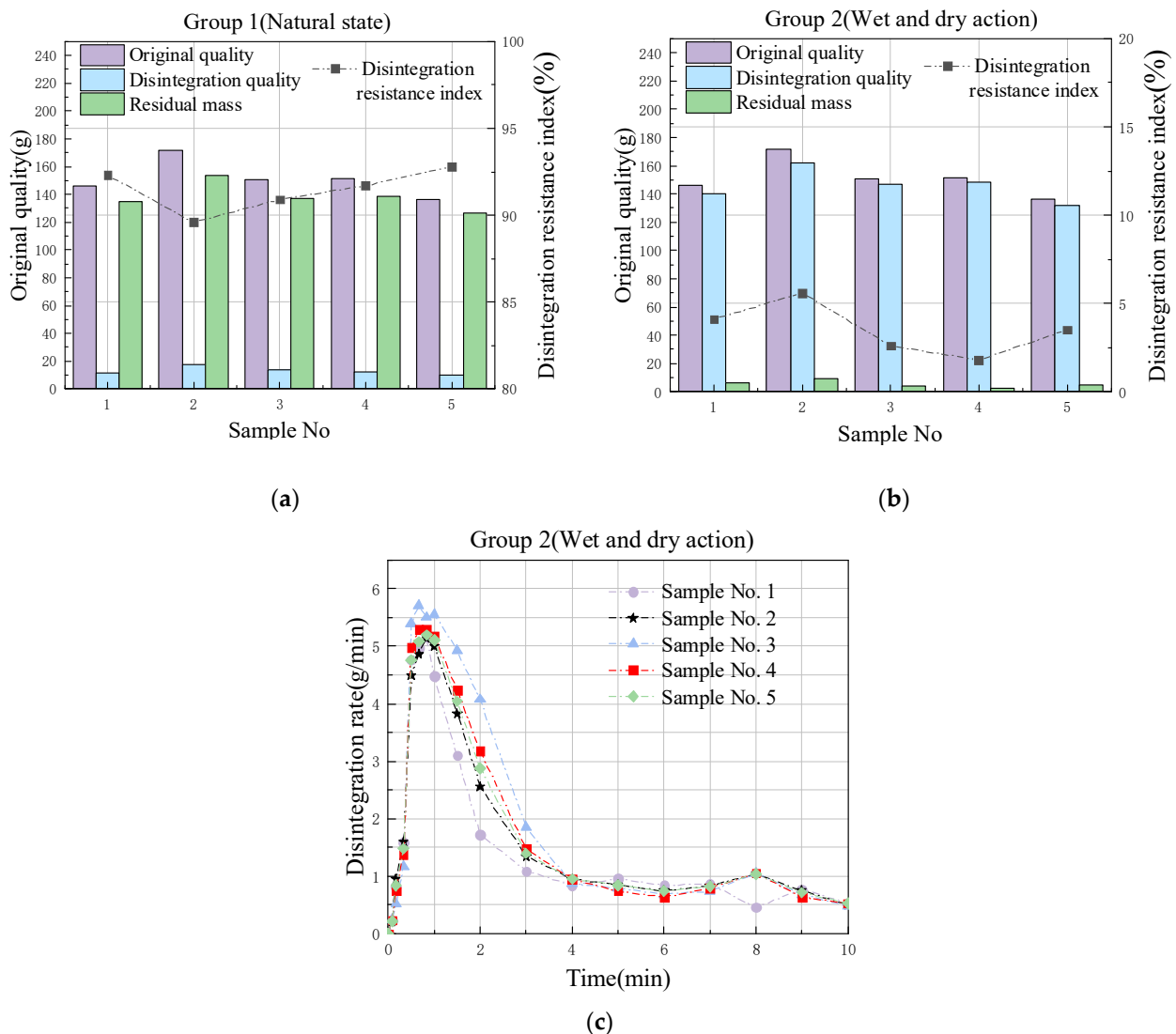


Figure 4. Disintegration test results of the two sets of samples: (a) comparison chart showing the disintegration resistance index values of the first group of samples; (b) comparison chart showing the disintegration resistance index values of the second group of samples; (c) comparison chart showing the disintegration rates of the first group of samples (average mass of 151.22 g).

4. Diatomaceous Earth Slope Tests

By combining the preliminary field investigation and indoor tests, it can be concluded that undisturbed diatomaceous earth has a high water content, high void ratio, and low permeability coefficient, and is often recognized as an impervious layer in the engineering

community. On the other hand, when the undisturbed diatomaceous earth loses water in the sun, cracks develop, and the diatomaceous earth disintegrates into lumps. The dried diatomaceous earth in the sun disintegrates quickly after being placed into water. This implies that the change in the water content is the most direct cause of the destruction of diatomaceous earth. Because this observation has not been analyzed and verified in conjunction with in situ tests, the resulting changes in soil deformation, soil pressure, and groundwater level in the slope soil are still unclear. Therefore, in order to obtain a more thorough understanding of the diatomaceous earth slope damage caused by alternating wet and dry conditions, two diatomaceous soil slopes with different slope ratios (1:1.5 and 1:2) in the test section were selected to conduct cycle simulations in the field, and comprehensive in situ monitoring and fissure observation of the slopes were carried out.

4.1. Simulation of Alternating Dry and Wet Cycles

4.1.1. Artificial Rainfall Simulation System for High-Speed Railway Slopes

To build an alternating dry and wet test environment for diatomaceous earth slopes, a convenient, efficient, and controllable high-speed railway slope artificial rainfall system was designed. The system mainly includes three parts, namely, the water supply module, control module, and rainfall module, as shown in Figure 5. The water supply module is used to provide a water source for the rainfall module, and the water supply module is connected to a control module. The control module is used to control the water supply intensity and flow rate of the water supply module, thereby controlling the rainfall process of the rainfall module. The rainfall module adopts a prefabricated rainfall bracket. Each rainfall bracket is composed of a ground anchor and a rainfall column with a pin bolt, which arbitrarily adjusts the height of the rainfall bracket and efficient installation, disassembly, and transportation. The rain sprinkler uses a detachable downward spray atomization sprinkler, which has two types of large diameters and small diameters that adjust the rainfall intensity and enrich the rainfall diversity. The control module controls the whole process of water supply and rainfall through a closed-loop control system composed of PU water pipes, valves, water meters, and pressure gauges, and its operation is simple and convenient. The water supply module stores and supplies water through water storage buckets, generators, water pumps, and water supply pipes.

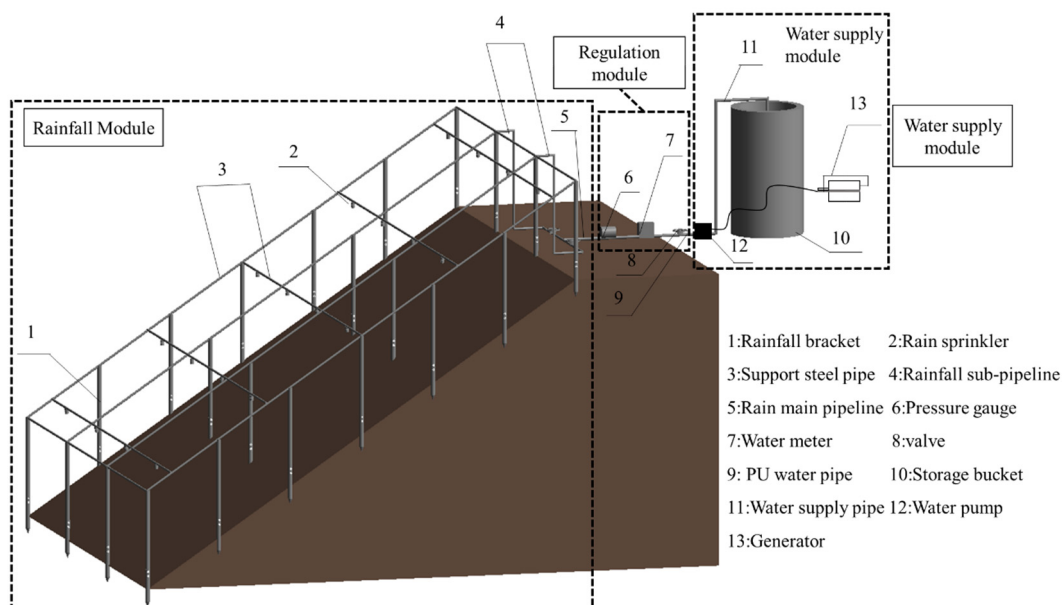


Figure 5. Schematic diagram of a convenient, efficient, and controllable high-speed railway slope artificial rainfall simulation system.

During use, the system can satisfactorily meet the needs of diatomaceous earth slopes to simulate artificial rainfall, match the intensity of natural rainfall, and achieve rainfall on slopes with different slope rates. The system has simple daily operations, easy disassembly and assembly, and easy transportation; it can be repeatedly tested at multiple test sites, which provides a strong guarantee for the development of high-speed rail projects. The actual installation and layout of the test site are shown in Figure 6.



Figure 6. Site installation of the rainfall system.

4.1.2. Test Plan of the Dry and Wet Cycle Simulation

The alternating dry and wet test process is shown in Table 3. In the field test, to simulate the effects of the dry and wet cycles in the natural environment, the rainfall was set to occur at night, and outside sunlight was used to evaporate water during the day, as shown in Figure 7a,b. On rainy days, to reduce the influence of rainwater on the rainfall test, a layer of colored striped cloth and a layer of plastic film were used to cover the supporting steel frame, as shown in Figure 7c.

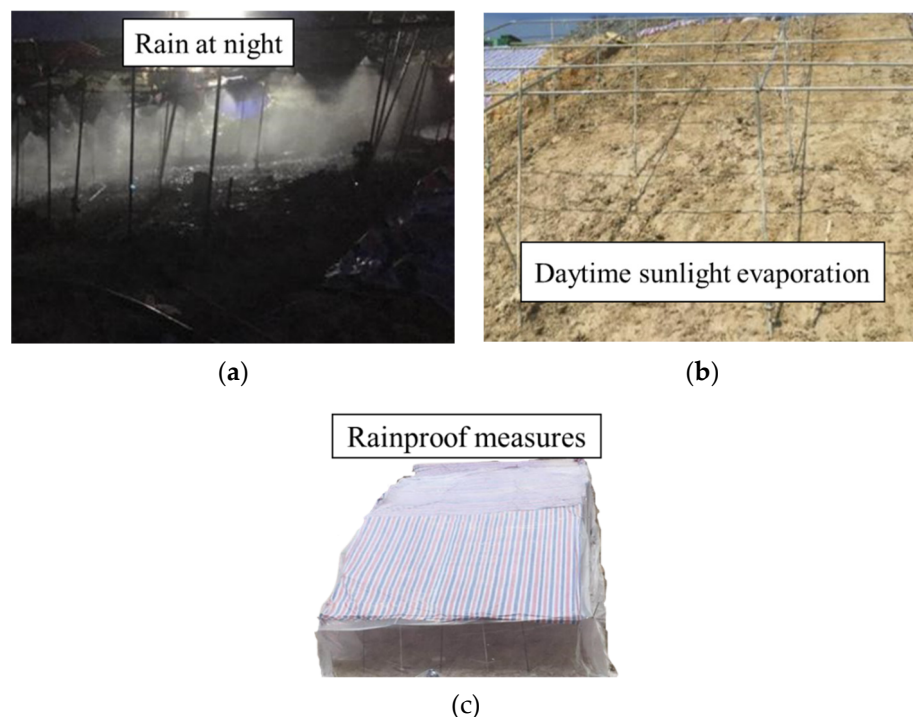


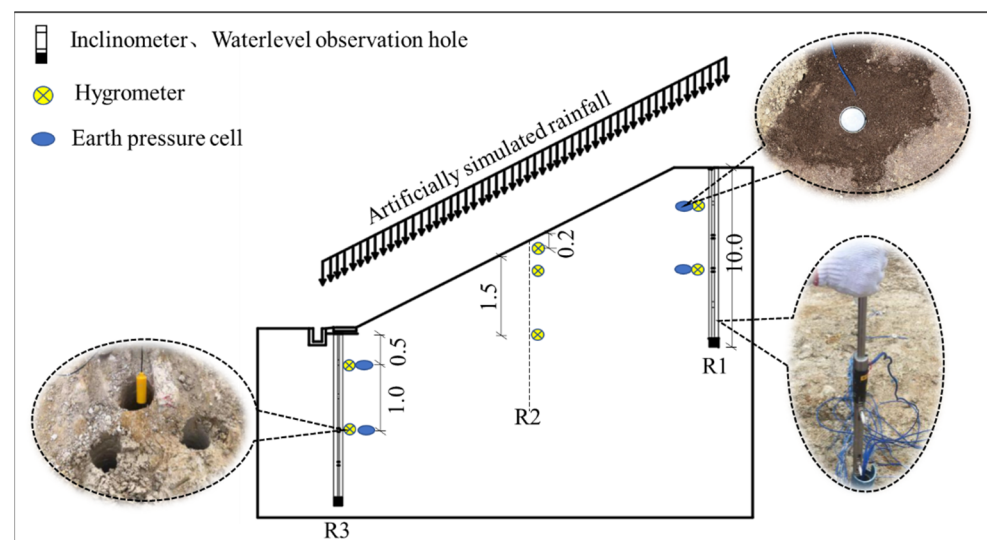
Figure 7. Dry and wet cycle simulation test: (a) rain at night; (b) dry during the day; (c) rainproof measures.

Table 3. Experimental history.

N°	Date	Test Slope	Rainfall Intensity	Daily Rainfall Time
1	27 June–2 July	1:2	8 mm/h	15 h
2	3 July–4 July	1:2	0 (Natural placement)	0
3	5 July–7 July	1:2	15 mm/h	15 h
4	13 July–18 July	1:1.5	8 mm/h	15 h
5	19 July–20 July	1:1.5	0	0
6	21 July–23 July	1:1.5	15 mm/h	15 h

4.2. In Situ Comprehensive Monitoring

Before and after the simulated rainfall test on the natural diatomaceous earth slope, comprehensive in situ monitoring was carried out. In the field test, the sensor layout of the two types of natural diatomaceous earth slope was the same, and monitoring profiles R1, R2, and R3 were positioned at the top, middle, and toe of the natural diatomaceous earth slope, respectively. Sensors were embedded at different depths to monitor the changes in the water content, horizontal displacement, earth pressure, and groundwater level of each profile, as shown in Figure 8.

**Figure 8.** Sensor layout (side view).

5. Results

5.1. Water Content Analysis

By reading the monitoring data of the automatic acquisition instrument, the monitored distribution pattern of the water contents in each section on the 1:2 slope and 1:1.5 slope are shown in Figure 9a,b, respectively. The results are summarized as follows:

1. Heavy rain and artificial simulated rainfall both led to an abrupt increase in the water content at each measuring point. For example, after the natural rainstorm on 18 June, the change in water content at the depth of 0.2 m on the slope of section R2 with a slope rate of 1:2 was the largest, changing from 48.1% to 59.4%—an increase of 11.3%—and the average value of the change in water content of each section was 4.4%. This indicates that rainfall has a significant impact on the water content at the measuring point. Before and after artificial simulated rainfall, on the slope with a slope ratio of 1:2, the water content at a depth of 1.5 m in the R1 section of the top of the slope increased the most—from 57.2% to 76.1%. On the slope with a slope ratio of 1:1.5, the water content at a depth of 1.5 m in the R2 section in the middle of the slope increased the most—from 58.8% to 78.9%. The reason for the sudden change in the water content was that the original

- structure of the diatomaceous earth was destroyed by the borehole construction at the measurement point [38], and the backfill was not dense, resulting in rapid infiltration after the rainfall began; thus, the water content increased abruptly;
2. The diatomaceous earth slope was excavated during artificial rainfall simulation, and rainfall infiltration was assessed. The diatomaceous earth flowed only within the range of 0.02–0.1 m from the surface of the slope, and the following diatomaceous earth structure was complete. Rainwater could not penetrate into the lower diatomite layer, and the measured water content was the same as that before rainfall, as shown in Figure 9c. This phenomenon is consistent with the results of the indoor hydraulic property observation test, again showing that natural diatomaceous earth experiences no obvious impact after encountering water;
 3. In the week before the end of the alternating dry–wet simulation, the water contents at 0.2 m on the two types of slopes remained stable, and subsequently fluctuated greatly. Approximately two and a half months after the end of the alternating dry and wet simulation, the water content at 0.5 m was greatly affected by the climate. The analysis shows that this occurred due to the initial fissures in the diatomaceous earth produced by the alternating dry and wet external environment. Over time, the fissures gradually developed from the surface of the slope to these two locations [39].
 4. After the alternating dry–wet simulation, the water contents at the top of the two types of slopes and at depth greater than 0.5 m remained stable, and the range of change was small, indicating that the soil at the measuring point reached a saturated state; this phenomenon is consistent with the analysis obtained by Zhao [40], and occurs due to the hindering of the evaporation of water vapor by the surface soil. Consequently, the lower soil is less affected by the natural environment, and the water content remains stable.

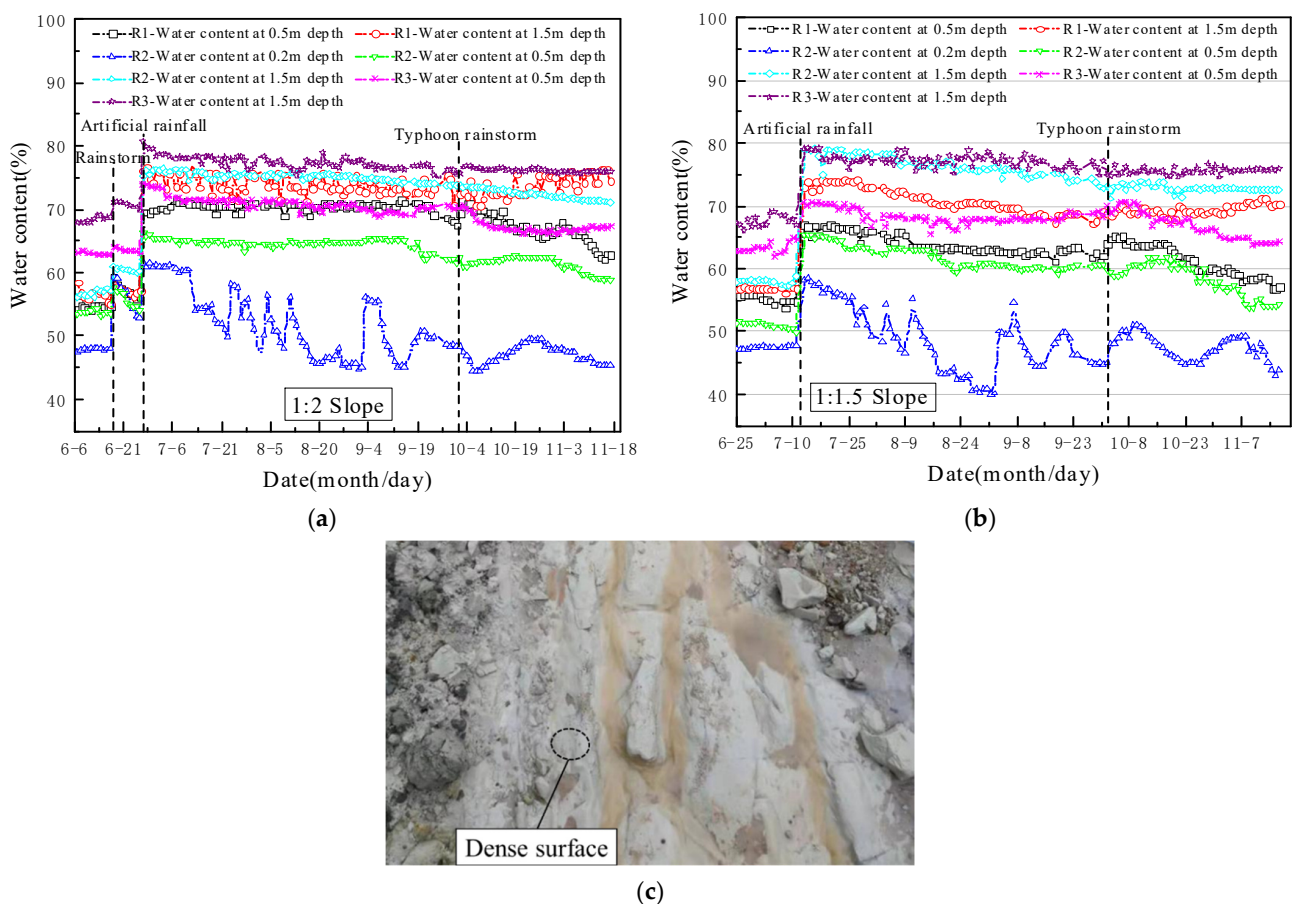


Figure 9. Water content analysis: (a) 1:2 natural slope water content variation trend; (b) 1:1.5 natural slope water content variation trend; (c) excavation of the diatomaceous earth slope.

5.2. Horizontal Displacement Analysis

By reading the monitoring data of the automatic acquisition instrument, the monitored horizontal displacement distribution of each section on the two types of slopes is shown in Figure 10a,b, and the following are indicated:

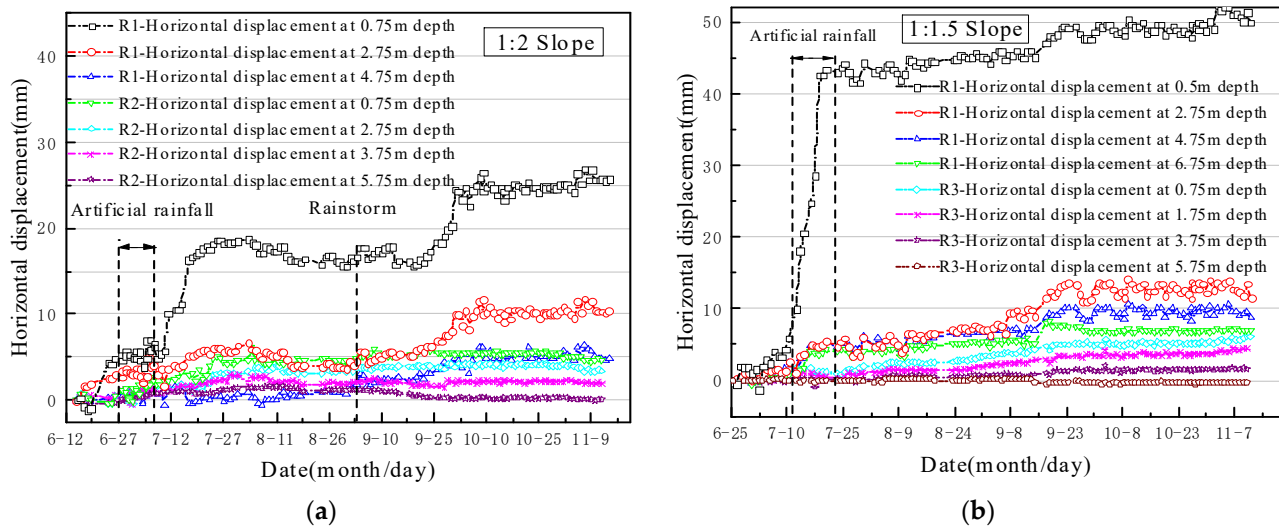


Figure 10. Horizontal displacement analysis: (a) 1:2 natural slope horizontal displacement variation trend; (b) 1:1.5 natural slope horizontal displacement variation trend.

On a slope with a ratio of 1:2, the monitored horizontal displacements at the depths of 0.75 m, 2.75 m, and 4.75 m at the top of the slope exhibited an overall increasing trend with depth, and were 25.7 mm, 10.8 mm, and 6.4 mm, respectively, after stabilization. However, during the dry–wet cycle simulation, the monitored horizontal displacement of the top of the 1:2 slope increased slightly, and a larger increase occurred after the rainfall ended, indicating that the monitored horizontal displacement of the 1:2 slope had a hysteresis effect relative to the rainfall; this phenomenon is similar to the landslide hysteresis effect of loess slopes obtained by Zhang [41]. After the dry–wet cycle simulation, the monitored horizontal displacements at the depths of 0.75 m and 2.75 m on the top of the slope increased to 20 mm and 6 mm, respectively, and temporarily stabilized. A heavy rainstorm occurred in the test area on 4 September, which resulted in a relatively large increase in the displacement of these two places on the slope. The displacement increased from 16.6 mm to 24.5 mm at 0.75 m depth and from 4.5 mm to 9.9 mm at 2.75 m depth, and stabilized at a later stage. However, the horizontal displacement at a depth of 4.75 m on the top of the slope was less affected by the environment, and was always in a relatively stable state, showing that the slope displacement mainly occurred between 0.75 m and 2.75 m from the surface, indicating shallow surface slip.

On a slope with a ratio of 1:1.5, the monitored horizontal displacements at the top of the slope at 0.75 m, 2.75 m, 4.75 m, and 6.75 m were 51.3 mm, 13.9 mm, 10.5 mm, and 7.4 mm, respectively. The horizontal displacement of the slope top mainly occurred on the shallow surface within 0.75–2.75 m, and the displacement increased abruptly at a depth of 0.75 m during the dry–wet cycle simulation. The main reason for this increase was that the slope with a ratio of 1:1.5 was relatively steep. After rainfall, the slope formed a relatively rapid current, which caused the shallow surface soil on the slope to produce larger displacements; this is consistent with the analysis obtained by Zhang [42]. The displacements of the slope top and the slope toe were not synchronized. The slope top displacement occurred only during the dry–wet cycle simulation, while the slope toe displacement continued to occur and gradually stabilized after 1 October. This phenomenon occurred because the top of the slope was mainly affected by the shallow surface displacement caused by rainfall, and the

foot of the slope was mainly affected by the overall displacement of the top of the slope, so it gradually stabilized in the later stage.

Comparing the 1:2 and 1:1.5 slopes, the horizontal displacement of the top surface of the 1:2 slope was much smaller than the horizontal displacement of the top surface of the 1:1.5 slope. The displacement difference between the surface layer and the bottom layer of the 1:2 slope was smaller than that of the 1:1.5 slope, indicating that the overall working performance of the 1:2 slope was stronger [43].

5.3. Lateral Earth Pressure Analysis

By reading the monitoring data of the automatic acquisition instrument, the monitored distribution pattern of the lateral earth pressure on each section of the 1:2 slope and 1:1.5 slope is shown in Figure 11a,b.

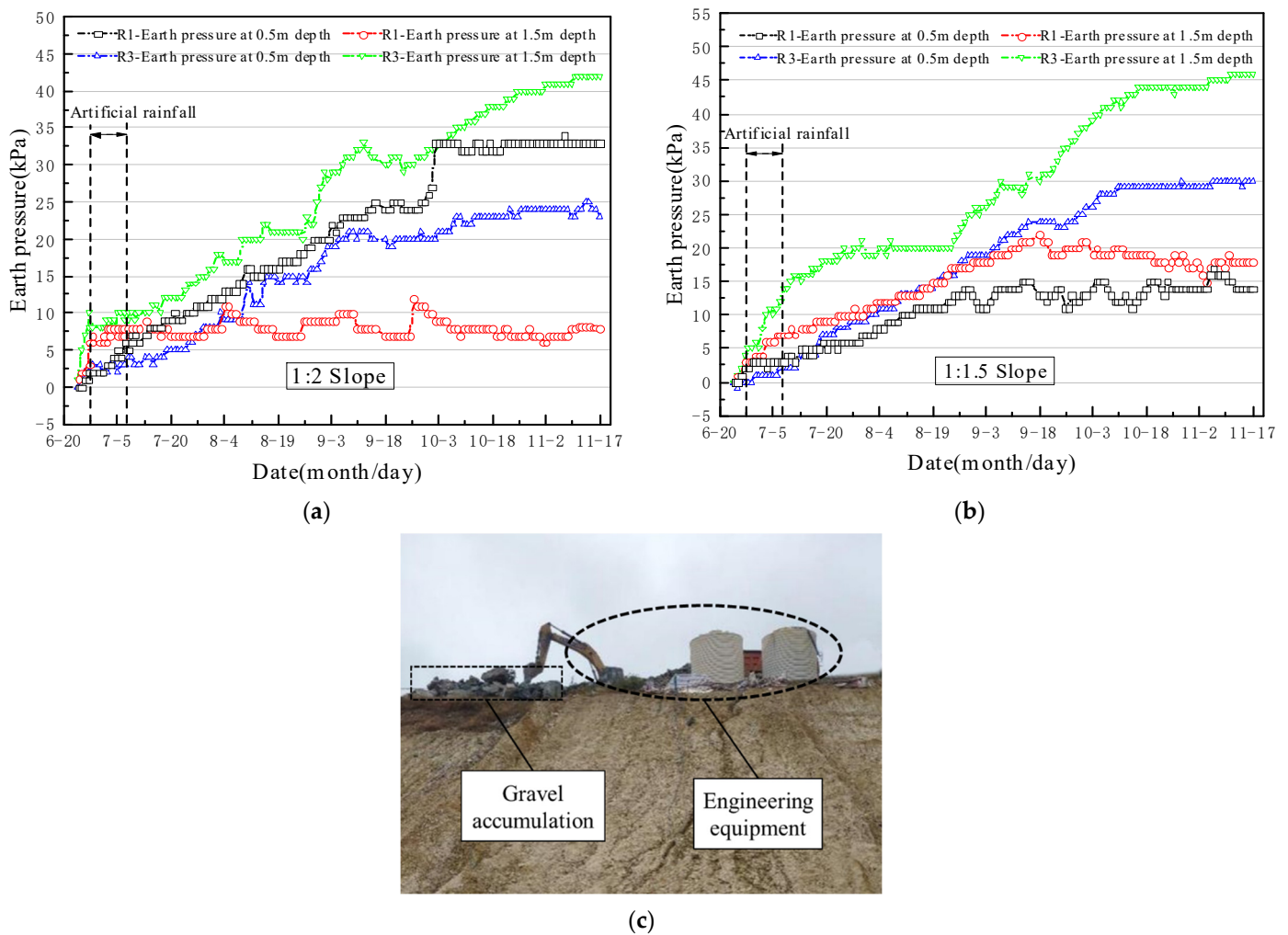


Figure 11. Lateral earth pressure analysis: (a) 1:2 natural slope lateral earth pressure variation trend; (b) 1:1.5 natural slope lateral earth pressure variation trend; (c) stacking on the top of the slope.

On a slope with a slope ratio of 1:2, the earth pressure at 0.5 m from the top of the slope continued to increase until it stabilized on 4 October, and the earth pressure at 1.5 m from the top of the slope gradually increased in the initial stage. Then, the earth pressure remained stable and experienced small fluctuations. The observations indicate that no significant change in earth pressure occurred after the artificial rainfall. An analysis of the reasons shows that artificial rainfall did not penetrate the slope, and had no effect on the internal earth pressure of the slope [44]. The earth pressure at the top of the slope at 0.5 m was greater than the earth pressure at the top of the slope at 1.5 m, mainly because of the

continuous accumulation of gravel on the top of the slope, which caused the earth pressure at the top of the slope to increase continuously [45]. The burial depth at 1.5 m was larger, and the impact of the piled load on it was small, as shown in Figure 11c.

On a slope with a ratio of 1:1.5, the lateral earth pressure at the top and toe of the slope both increased in the early stage, and gradually stabilized in the later stage. However, the R1 section at the top of the slope still fluctuated slightly after being stabilized. It may be the case that the piled load on the top of the slope tended to be stable in the later stage; however, every day, there were new abandoned slags, and some of the abandoned slags were used for filling; thus, a small fluctuation in the stacking load occurred, as shown in Figure 11c. An analysis of the earth pressure during artificial rainfall simulation showed that the artificial rainfall had no obvious impact on the 1:1.5 slope, indicating that the artificial rainfall did not penetrate into the interior of the 1:1.5 slope.

5.4. Groundwater Level Analysis

The groundwater level observation point of the test site was buried 6.5 m below the toe of the slope. As shown in Figure 12, no significant change in the groundwater level occurred before or after rainfall. The figure shows that the rainfall did not penetrate into the diatomaceous soil slope, and the groundwater level did not rise overall [46,47].

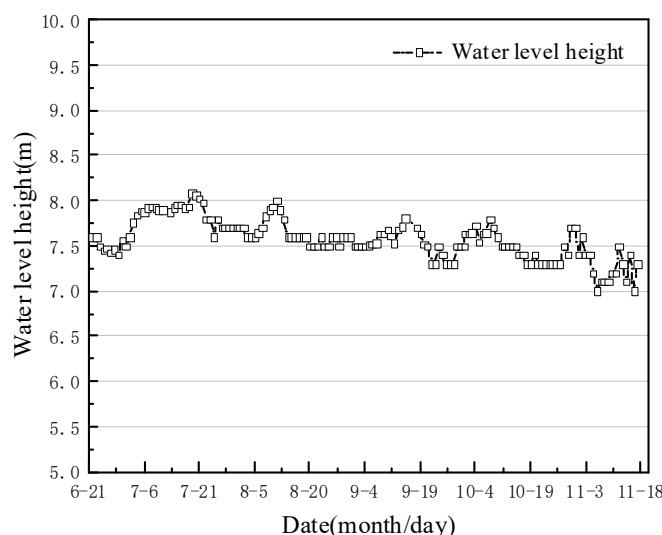


Figure 12. Groundwater level change.

5.5. Crack Analysis

To study the process of crack development in diatomaceous earth under the action of an external environment, it is necessary to constantly observe the changes in cracks during the test. Field observations and measurements after the end of the test showed that the crack widths of the 1:2 slope were 10–25 mm, and the crack depths were 50–60 cm, while for the 1:1.5 slope, the widths of the cracks in the slope were 10–20 mm, and the depths of the cracks were 40–55 cm, as shown in Figure 13. The development process of the above cracks was as follows:

Diatomaceous earth has a high water content and low permeability [48,49]. Natural diatomaceous earth with a high water content after slope excavation is exposed to the natural environment, and water evaporates quickly under sunlight. Due to the high surface temperature, the water evaporates quickly, the internal diatomaceous earth is affected by the surface layer, and the water of that layer has difficulty evaporating, resulting in a large difference in the upper and lower water contents, and leading to initial cracks [50,51]. Under the action of rainfall, the surface diatomaceous earth forms a hard shell layer because of rainwater, and the rainwater enters the cracks, which intensifies the development of the cracks. Because of evaporation, the fissures develop rapidly, and the integral diatomaceous

earth slope is cut into several small pieces. This process is consistent with the above water physical property test results of diatomaceous earth. Because diatomaceous earth has a certain bedding structure, diatomaceous earth disintegrates from a monolithic soil layer into large rocks because of evaporation. Then, it breaks down into small rocks, which intensifies the infiltration of rainwater. If this process continues, under long-term alternating dry and wet conditions, the shallow diatomaceous soil is completely disintegrated, and residual soil is formed at the foot of the slope because of rainfall. The failure mode of the slope is shallow instability failure, as shown in Figure 14.

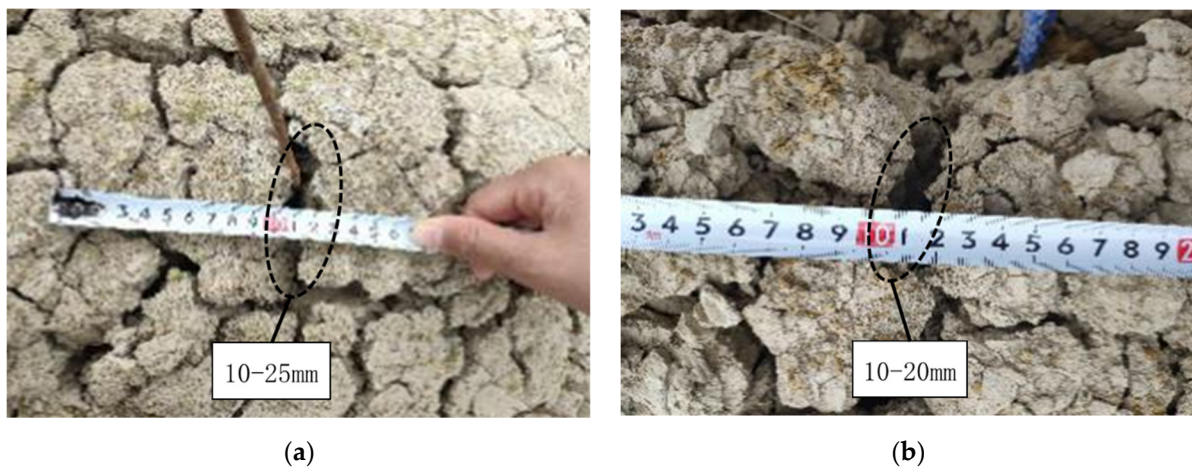


Figure 13. Slope fissure diagram: (a) test section on the 1:2 side slope; (b) test section on the 1:1.5 side slope.



Figure 14. Natural side slope observation map.

6. Conclusions

In this paper, based on the newly built Hangzhou–Taizhou high-speed railway diatomaceous earth natural slope test section, indoor tests, in situ comprehensive monitoring, and fissure observation, as well as other methods, the following conclusions were obtained:

1. The hydrological properties of diatomaceous earth in the Shengzhou area are extremely poor, and natural diatomaceous earth samples do not change significantly when exposed to water. The disintegration resistance index values are 89.6–92.8%, and the disintegration resistance is strong. After the natural diatomaceous earth samples were dried in the shade, cracks appeared and fragmentation occurred due to dry–wet cycle effects. Then, the samples disintegrated rapidly when exposed to water, with disintegration resistance index values of 1.8–5.6% and an average value of 3.7%. The disintegration resistance was very weak, and the disintegration was strong;
2. A convenient, efficient, and controllable high-speed railway slope artificial rainfall simulation system was designed to provide strong support for the development of

alternating dry and wet simulations. During the artificial rainfall simulation period, the diatomaceous earth was in a flowing state within the range of 0.02–0.1 m from the surface of the slope, and rainwater could not seep into the soil. After the alternating dry–wet simulation, cracks developed within the range of 0–0.5 m on the slope, and the water content was greatly affected by the environment. Comprehensive indoor water physical property observations and water content monitoring results show that natural diatomaceous earth has no obvious impact when exposed to water, but it disintegrates and cracks under the action of alternating dry and wet cycles;

3. For the 1:2 diatomaceous earth slope, the monitored horizontal displacements at depths of 0.75 m, 2.75 m, and 4.75 m at the top of the slope were 25.7 mm, 10.8 mm, and 6.4 mm, respectively; for the 1:1.5 diatomaceous earth slope, the monitored horizontal displacements at the depths of 0.75 m, 2.75 m, and 4.75 m at the top of the slope were 51.3 mm, 13.9 mm, and 10.5 mm, respectively; The horizontal displacement of the two types of slopes mainly occurred on the surface within 0.75–2.75 m, indicating shallow slip;
4. After the test, the crack widths of the natural diatomaceous earth slope reached 10–25 mm, and the depth reached 40–60 cm. The natural slope of diatomaceous earth is prone to complete disintegration of shallow soil under the effect of long-term alternating wet and dry conditions, and residual soil is formed at the foot of the slope under the effect of rainfall, resulting in shallow destabilization damage, which greatly affects the safe development of railroad construction;
5. The key to preventing the damage to diatomaceous earth slopes is to protect the original diatomaceous earth, isolate the alternating dry and wet effects of the outside atmosphere on the surface layer of the diatomaceous earth slope, prevent the original diatomaceous earth from producing a water content gradient, and avoid the fissure of the surface layer of the diatomaceous earth slope. In the actual high-speed railroad construction, it is recommended to provide proper protection for diatomite slopes.

Because of the limited number of research years of the authors, the issues that can be further studied in the future are as follows:

1. Since the monitoring time of the field test is too short and the alternating wet and dry action fails to fully develop the slope fissures, it is suggested to monitor the diatomite slope for ~3 years in order to further quantify the influence range of diatomite fissures, and to monitor the displacement, water content, pore water pressure, earth pressure, and groundwater level changes for a long time;
2. On-site fissure diatomite strength tests should be conducted to provide strong support for analyzing the influence of fissures on the stability of diatomite slopes, and the influence of rainfall scouring on the stability of diatomite slopes should be considered;
3. Further numerical simulation and theoretical analysis of diatomite slope stability under the action of alternating wet and dry conditions should be carried out.

Author Contributions: Conceptualization, W.W. and Z.D.; methodology, Z.D.; software, Z.D.; validation, Z.D., W.W. and T.Y.; formal analysis, Z.D.; investigation, Q.S.; resources, Y.L. (Yandong Li); data curation, W.W. and Y.L. (Yangyang Liu); writing—original draft preparation, W.W. and Z.D.; writing—review and editing, Z.D. and K.X.; visualization, Q.S.; supervision, T.Y.; project administration, T.Y.; funding acquisition, Q.S. All authors have read and agreed to the published version of the manuscript.

Funding: This research was funded by China Railway Construction Co., Ltd., under grant no. 2018-A01, and the National Natural Science Foundation of China, grant number 51978588.

Institutional Review Board Statement: Not applicable.

Informed Consent Statement: Not applicable.

Data Availability Statement: Not applicable.

Conflicts of Interest: The authors declare no conflict of interest.

References

- Day, R.B. Engineering properties of diatomaceous fill. *J. Geotech. Eng.* **1995**, *121*, 908–910. [[CrossRef](#)]
- Tateishi, Y. Geotechnical Properties of Diatom Earth and Stability of Surface Layer for the Cut Slope. Ph.D. Thesis, Saga University, Saga City, Japan, 1997.
- Shigematsu, H.; Yashima, A.; Nishio, M.; Saka, Y.; Hatanaka, S. Geotechnical properties of diatomaceous earth in northern gifu prefecture and cut slope stability. *Doboku Gakkai Ronbunshu* **2001**, *2001*, 139–154. [[CrossRef](#)]
- Díaz-Rodríguez, J.; González-Rodríguez, R. Influence of diatom microfossils on soil compressibility. In Proceedings of the 18th International Conference on Soil Mechanics and Geotechnical Engineering, Paris, France, 2–5 September 2013.
- Caicedo, B.; Mendoza, C.; López, F.; Lizcano, A. Behavior of diatomaceous soil in lacustrine deposits of Bogotá, Colombia. *Rock Mech. Geotech. Eng.* **2018**, *10*, 367–379. [[CrossRef](#)]
- Ovalle, C.; Arenaldi-Perisic, G. Mechanical behaviour of undisturbed bed diatomaceous soil. *Mar. Georesources Geotechnol.* **2021**, *39*, 623–630. [[CrossRef](#)]
- Chu, H.; Cao, D.; Dong, B.; Qiang, Z. Bio-diatomite dynamic membrane reactor for micro-polluted surface water treatment. *Water Res.* **2010**, *44*, 1573–1579. [[CrossRef](#)]
- Jeffryes, C.; Campbell, J.; Li, H.; Jiao, J.; Rorrer, G. The potential of diatom nanobiotechnology for applications in solar cells, batteries, and electroluminescent devices. *Energy Environ. Sci.* **2011**, *4*, 3930–3941. [[CrossRef](#)]
- Liu, D.; Gu, J.; Liu, Q.; Tan, Y.; Li, Z.; Zhang, W.; Su, Y.; Li, W.; Cui, A.; Gu, C.; et al. Metal-Organic Frameworks Reactivate Deceased Diatoms to be Efficient CO₂Absorbents. *Adv. Mater.* **2013**, *26*, 1229–1234. [[CrossRef](#)]
- Li, J.; Xu, J.; Xie, Z.; Gao, X.; Zhou, J.; Xiong, Y.; Chen, C.; Zhang, J.; Liu, Z. Diatomite-Templated Synthesis of Freestanding 3D Graphdiyne for Energy Storage and Catalysis Application. *Adv. Mater.* **2018**, *30*, e1800548. [[CrossRef](#)] [[PubMed](#)]
- Zhou, F.; Li, Z.; Lu, Y.-Y.; Shen, B.; Guan, Y.; Wang, X.-X.; Yin, Y.-C.; Zhu, B.-S.; Lu, L.-L.; Ni, Y.; et al. Diatomaceous Earth derived hierarchical hybrid anode for high performance all-solid-state lithium metal batteries. *Nat. Commun.* **2019**, *10*, 1–11.
- Tu, X.B.; Kwong, A.F.L.; Dai, F.C.; Tham, L.G.; Min, H. Field monitoring of rainfall infiltration in a loess slope and analysis of failure mechanism of rainfall-induced landslides. *Eng. Geol.* **2009**, *105*, 134–150. [[CrossRef](#)]
- Ye, W.; Zhang, Y. Effect of Dry-wet Cycle on the Formation of Loess Slope Spalling Hazards. *Civ. Eng. J.* **2018**, *4*, 785. [[CrossRef](#)]
- Yates, K.; Russell, A.; Fenton, C. Field and laboratory investigation of rainfall-triggered slope failure in unsaturated loess soils, New Zealand. *E3S Web Conf.* **2020**, *195*, 01017. [[CrossRef](#)]
- Xu, J.; Ren, C.; Wang, S.; Gao, J.; Zhou, X. Permeability and Microstructure of a Saline Intact Loess after Dry-Wet Cycles. *Adv. Civ. Eng.* **2021**, *2021*, 6653697. [[CrossRef](#)]
- Zeng, Z.T.; Lu, H.B.; Zhao, Y.L. Wetting-Drying Effect of Expansive Soils and its Influence on Slope Stability. *Appl. Mech. Mater.* **2012**, *170–173*, 889–893. [[CrossRef](#)]
- Xiao, J.; Yang, H.; Zhang, J.; Tang, X. Surficial failure of expansive soil cutting slope and its flexible support treatment technology. *Adv. Civ. Eng.* **2018**, *2018*, 1609608. [[CrossRef](#)]
- Chen, T.-L.; Zhou, C.; Wang, G.-L.; Liu, E.-L.; Dai, F. Centrifuge Model Test on Unsaturated Expansive Soil Slopes with Cyclic Wetting–Drying and Inundation at the Slope Toe. *Int. J. Civ. Eng.* **2017**, *16*, 1341–1360. [[CrossRef](#)]
- Zhai, J.-Y.; Cai, X.-Y. Strength Characteristics and Slope Stability of Expansive Soil from Pingdingshan, China. *Adv. Mater. Sci. Eng.* **2018**, *2018*, 3293619. [[CrossRef](#)]
- Perisic, G.A.; Ovalle, C.; Barrios, A. Antonio Barrios. Compressibility and creep of a diatomaceous soil. *Eng. Geol.* **2019**, *258*, 105145. [[CrossRef](#)]
- Hong, Z.; Tateishi, Y.; Han, J. Experimental study of macro-and microbehavior of natural Diatomaceous Earth. *J. Geotech. Geoenviron. Eng.* **2006**, *132*, 603–610. [[CrossRef](#)]
- Zhang, Y.; Guo, C.; Yao, X.; Qu, Y.; Zhou, N. Engineering geological characterization of clayey diatomaceous earth deposits encountered in highway projects in the Tengchong region, Yunnan, China. *Eng. Geol.* **2013**, *167*, 95–104. [[CrossRef](#)]
- Shiwakoti, D.R.; Tanaka, H.; Tanaka, M.; Locat, J. Influences of Diatom Microfossils on Engineering Properties of Soils. *Soils Found.* **2002**, *42*, 1–17. [[CrossRef](#)]
- Wiemer, G.; Dziadek, R.; Kopf, A. The enigmatic consolidation of diatomaceous sediment. *Mar. Geol.* **2017**, *385*, 173–184. [[CrossRef](#)]
- Guo, C.; Zhou, N.; Fu, X.; Zhang, Y.; Zhang, R. The optimization design of the research on the formation mechanism, prevention and control of landslide along clayey diatomite highway in Tengchong, Yunnan Pzovince. *Geol. Bul. China* **2013**, *32*, 2021–2030. (In Chinese)
- Wiemer, G.; Moernaut, J.; Stark, N.; Kempf, P.; De Batist, M.; Pino, M.; Urrutia, R.; De Guevara, B.L.; Strasser, M.; Kopf, A. The role of sediment composition and behavior under dynamic loading conditions on slope failure initiation: A study of a subaqueous landslide in earthquake-prone South-Central Chile. *Geol. Rundsch.* **2015**, *104*, 1439–1457. [[CrossRef](#)]
- Ministry of Railways of the People’s Republic of China. *Geotechnical Test Procedures for Railroad Engineering (TB10102-2004)*; China Railway Press: Beijing, China, 2004. (In Chinese)
- Zhang, Y.; Qu, Y.; Liu, G.; Wu, S. Engineering geological properties of Miocene hard clays along the middle line of the North–South Diversion Water Project in China. *Bull. Eng. Geol. Environ.* **2003**, *62*, 213–219. [[CrossRef](#)]
- Leng, T.; Tang, C.; Li, D.; Li, Y.; Zhang, Y.; Wang, K.; Shi, B. Advance on the engineering geological characteristics of expansive soil. *J. Eng. Geol.* **2018**, *26*, 112–128. (In Chinese)

30. Tang, C.; Shi, B.; Liu, C. Study on desiccation cracking behaviour of expansive soil. *J. Eng. Geol.* **2012**, *20*, 663–673. (In Chinese)
31. Zhang, Y.; Guo, C.; Qu, Y.; Yao, X. Research on mechanical properties of swelling diatomite and their geohazard effects. *Rock Soil Mech.* **2013**, *34*, 23–30. (In Chinese)
32. Guo, C.; Zhang, Y.; Meng, Q.; Zheng, G.; Li, H. Research on shear strength of remolding diatomite by ring shear tests. *Rock Soil Mech.* **2013**, *34*, 92–100. (In Chinese)
33. Zhang, Y.; Guo, C.; Qu, Y.; Zhang, M. Discovery of swelling diatomite at tengchong, yunnan province and its implication in engineering geology. *J. Eng. Geol.* **2012**, *20*, 266–275. (In Chinese)
34. Tang, J.; Yu, P.; Wei, H.Z.; Meng, Q.S. Slaking behaviour of weathered basalt residual soil in guizhou. *J. Eng. Geol.* **2011**, *19*, 778–783. (In Chinese)
35. Zhang, Z.; Liu, W.; Cui, Q.; Han, L.; Yao, H. Disintegration characteristics of moderately weathered mudstone in drawdown area of Three Gorges Reservoir, China. *Arab. J. Geosci.* **2018**, *11*, 405. [[CrossRef](#)]
36. Li, C.; Kong, L.; Shu, R.; An, R.; Zhang, X. Disintegration characteristics in granite residual soil and their relationship with the collapsing gully in South China. *Open Geosci.* **2020**, *12*, 1116–1126. [[CrossRef](#)]
37. Luo, X.; Gao, H.; He, P.; Liu, W. Experimental investigation of dry density, initial moisture content, and temperature for granite residual soil disintegration. *Arab. J. Geosci.* **2021**, *14*, 1–9. [[CrossRef](#)]
38. Zhou, S.; Tian, Z.; Di, H.; Guo, P.; Fu, L. Investigation of a loess-mudstone landslide and the induced structural damage in a high-speed railway tunnel. *Bull. Eng. Geol. Environ.* **2020**, *79*, 2201–2212. [[CrossRef](#)]
39. Zhang, J.-M.; Luo, Y.; Zhou, Z.; Chong, L.; Victor, C.; Zhang, Y.-F. Effects of preferential flow induced by desiccation cracks on slope stability. *Eng. Geol.* **2021**, *288*, 106164. [[CrossRef](#)]
40. Zhao, Y.; Feng, J.; Liu, K.; Xu, H.; Wang, L.; Liu, H. Study of the Stability of a Soil-Rock Road Cutting Slope in a Permafrost Region of Hulunbuir. *Adv. Civ. Eng.* **2020**, *2020*, 6701958. [[CrossRef](#)]
41. Zhang, S.; Zhang, X.; Pei, X.; Wang, S.; Huang, R.; Xu, Q.; Wang, Z. Model test study on the hydrological mechanisms and early warning thresholds for loess fill slope failure induced by rainfall. *Eng. Geol.* **2019**, *258*, 105135. [[CrossRef](#)]
42. Zhang, G.; Wang, R.; Qian, J.; Zhang, J.-M.; Qian, J. Effect study of cracks on behavior of soil slope under rainfall conditions. *Soils Found.* **2012**, *52*, 634–643. [[CrossRef](#)]
43. Yang, Z.; Lv, J.; Shi, W.; Zhang, Q.; Lu, Z.; Zhang, Y.; Ling, X. Model Test Study on Stability Factors of Expansive Soil Slopes with Different Initial Slope Ratios under Freeze-Thaw Conditions. *Appl. Sci.* **2021**, *11*, 8480. [[CrossRef](#)]
44. Chang, Z.; Huang, F.; Huang, J.; Jiang, S.-H.; Zhou, C.; Zhu, L. Experimental study of the failure mode and mechanism of loess fill slopes induced by rainfall. *Eng. Geol.* **2020**, *280*, 105941. [[CrossRef](#)]
45. Hou, H.-J.; Wang, B.; Deng, Q.-X.; Zhu, Z.-W.; Xiao, F. Model Experimental Study on Stress Transfer and Redistribution in a Clay Landslide under Surcharge Load. *Adv. Mater. Sci. Eng.* **2020**, *2020*, 4269043. [[CrossRef](#)]
46. Krisnanto, S.; Rahardjo, H.; Kartiko, R.D.; Satyanaga, A.; Nugroho, J.; Mulyanto, N.; Rachma, S.N. Characteristics of Rain-fall-Induced Slope Instability in Cisokan Region, Indonesia. *J. Eng. Technol. Sci.* **2021**, *53*, 1–21. [[CrossRef](#)]
47. Hamdhan, I.; Schweiger, H. Finite element method-based analysis of an unsaturated soil slope subjected to rainfall infiltration. *Int. J. Geomech.* **2013**, *13*, 653–658. [[CrossRef](#)]
48. Chaika, C.; Dvorkin, J. Porosity Reduction During Diagenesis of Diatomaceous Rocks. *AAPG Bull.* **2000**, *84*, 1173–1184. [[CrossRef](#)]
49. Burger, C.A.; Shackelford, C.D. Soil-Water Characteristic Curves and Dual Porosity of Sand–Diatomaceous Earth Mixtures. *J. Geotech. Geoenviron. Eng.* **2001**, *127*, 790–800. [[CrossRef](#)]
50. Wu, L.Z.; Zhang, L.M.; Zhou, Y.; Xu, Q.; Yu, B.; Liu, G.G.; Bai, L.Y. Theoretical analysis and model test for rainfall-induced shallow landslides in the red-bed area of Sichuan. *Bull. Eng. Geol. Environ.* **2017**, *77*, 1343–1353. [[CrossRef](#)]
51. Li, Q.; Wang, Y.M.; Zhang, K.B.; Yu, H.; Tao, Z.Y. Field investigation and numerical study of a siltstone slope instability induced by excavation and rainfall. *Landslides* **2020**, *17*, 1485–1499. [[CrossRef](#)]